

Explanation of Temporal Clustering of Tsunami Sources Using the Epidemic-Type Aftershock Sequence Model

by Eric L. Geist

Abstract Temporal clustering of tsunami sources is examined in terms of a branching process model. It previously was observed that there are more short interevent times between consecutive tsunami sources than expected from a stationary Poisson process. The epidemic-type aftershock sequence (ETAS) branching process model is fitted to tsunami catalog events, using the earthquake magnitude of the causative event from the Centennial and Global Centroid Moment Tensor (CMT) catalogs and tsunami sizes above a completeness level as a mark to indicate that a tsunami was generated. The ETAS parameters are estimated using the maximum-likelihood method. The interevent distribution associated with the ETAS model provides a better fit to the data than the Poisson model or other temporal clustering models. When tsunamigenic conditions (magnitude threshold, submarine location, dip-slip mechanism) are applied to the Global CMT catalog, ETAS parameters are obtained that are consistent with those estimated from the tsunami catalog. In particular, the dip-slip condition appears to result in a near zero magnitude effect for triggered tsunami sources. The overall consistency between results from the tsunami catalog and that from the earthquake catalog under tsunamigenic conditions indicates that ETAS models based on seismicity can provide the structure for understanding patterns of tsunami source occurrence. The fractional rate of triggered tsunami sources on a global basis is approximately 14%.

Online Material: Figures of residual analysis for tsunami and earthquake catalogs.

Introduction

Temporal clustering of tsunami events beyond what is expected from a Poisson process has been demonstrated in previous studies (Geist and Parsons, 2008, 2011; Geist, 2012). These studies are largely empirical in nature, though a cursory examination of the sources (Geist and Parsons, 2011) suggests that both aftershocks on the same fault and triggered events on different faults contribute to the temporal clusters. Geist and Parsons (2011) provisionally identified clusters of tsunami sources based on simple interevent time and spatial criteria. It is likely that tsunami source clusters are more extensive in time and space than described in Geist and Parsons (2011). A more objective and systematic analysis of tsunami source clustering based on event-to-event triggering is needed, such as has been developed for earthquakes (e.g., Zhuang *et al.*, 2002). Toward this objective, I examine in this paper whether a branching process based on the statistics for earthquake triggering can be used to explain the observed temporal clustering of tsunami sources.

Tsunami-generating events are viewed in this study as a point process—specifically, as random point sequences along the time axis. The point process is defined by the origin time of the earthquake and is marked by both earthquake

magnitude (from earthquake catalogs) and maximum-per-event tsunami size (i.e., the maximum amplitude or runup listed for an event in the tsunami catalog). Branching processes are a type of Markov process that has been explored in detail for earthquakes (Kagan, 1973a,b; Vere-Jones, 1976; Ogata, 1988, 1998). It is assumed that there is stochastic dependence among points in a cluster and that these points are not the result of random heterogeneity. The rate of triggered events depends on the magnitude of the parent event and the elapse time since that event. Tsunami size is only used as a mark for determining a tsunami-generating event, according to a minimum completeness level. Tsunami size is dependent on the earthquake magnitude; however, because tsunami size is only used as an indicator of tsunamigenesis, the issue of dependent marks is not explored in this study. Of the various branching process models, the epidemic-type aftershock sequence (ETAS) model (Ogata, 1988) is commonly used to explain many different aspects of seismicity and is the model used in this study. The space–time version of the ETAS model (Ogata, 1998) is not used in this study because of the paucity of tsunami events in the historical catalog compared to earthquakes. Other cluster processes,

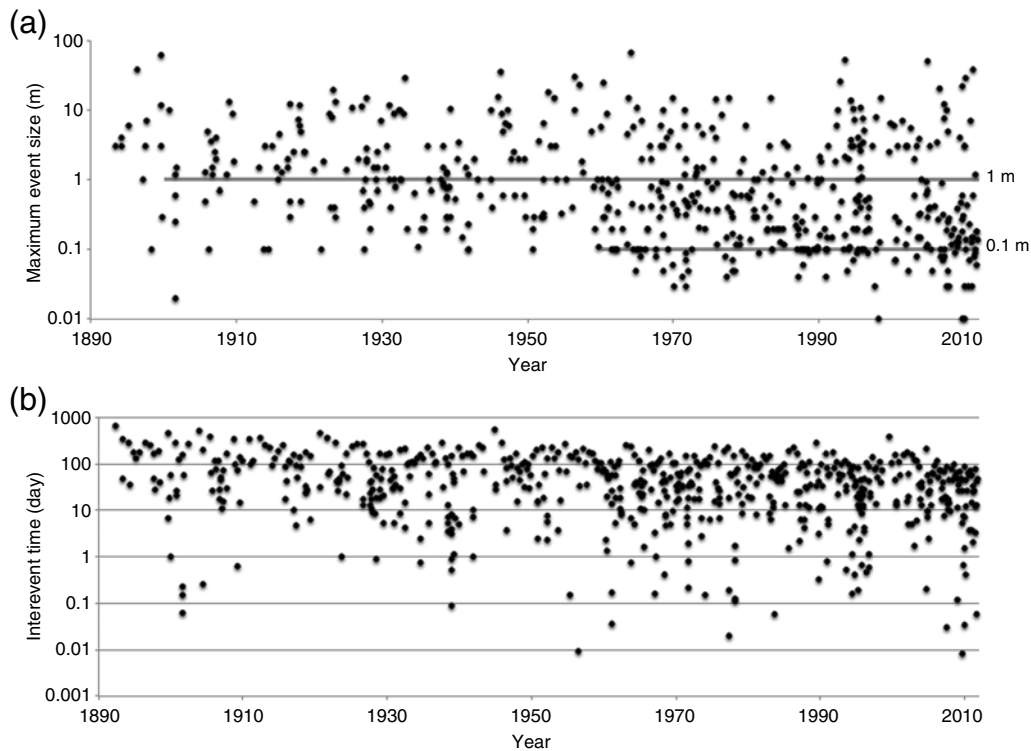


Figure 1. Tsunami catalog from 1890 to 2012. (a) Maximum size of each event plotted on logarithmic scale. The horizontal lines indicate duration of catalog completeness for two minimum levels (0.1 and 1 m). (b) Interevent time between successive events plotted on a logarithmic scale.

such as the Neyman–Scott process (Vere-Jones, 1970; Kagan, 1973b), may be equally successful in explaining the temporal occurrence of tsunami sources, although the wide use of the ETAS model in describing seismicity lends itself to providing a foundation for various applications (e.g., declustering, forecasting, etc.).

In addition to determining ETAS parameters for the catalog of tsunami events described above, parameters also are estimated for different earthquake catalogs under theoretical tsunamigenic conditions. We generally have a good understanding of the conditions in which earthquakes generate tsunamis; namely, there has to be sufficient vertical displacement of the water column to generate surface gravity waves. The primary tsunamigenic conditions examined in this study are (1) submarine location, (2) minimum threshold magnitude, (3) maximum focal depth, and (4) a dominant dip-slip component of fault motion. The latter three conditions scale to minimum peak vertical displacement of the seafloor.

This study is organized as follows. First, empirical analysis of tsunami catalog data that exhibit temporal clustering is reviewed. Then, the ETAS model developed for seismicity is reviewed, along with a description of the maximum-likelihood method used for estimating the ETAS parameters. ETAS results are first provided for the tsunami catalog, updated by cross referencing earthquake magnitudes to the Centennial and Global Centroid Moment Tensor (CMT) catalogs. I then determine if these parameters are consistent with ETAS parameters

estimated from earthquake catalogs under different tsunamigenic conditions. Results of the foregoing analysis are discussed with particular attention to how the tsunamigenic conditions affect the estimation of the ETAS parameters.

Evidence for Temporal Clustering of Tsunamis

Temporal clustering of tsunami sources can be demonstrated by plotting the distribution of observed interevent times. Figure 1 shows the maximum-per-event sizes and interevent times for all tsunami events from 1890 through 2012 from the National Geophysical Data Center (NGDC) tsunami event database. In Figure 2, interevent times from 1960 to 2012 with a completeness size of 0.1 m are binned according to the exponential function $\Delta\tau^n n = 1, 2, 3, \dots$, in which the binning parameter $\Delta\tau$ is consistent with the range of the data (Corral, 2004) and is plotted on a log–log scale. The heavy solid line indicates the exponential distribution associated with a stationary Poisson process. As indicated by the binned observations in Figure 2, there are more short interevent times than predicted by a Poisson process. Because of the relatively high-magnitude threshold for tsunamigenesis ($M \sim 7$), however, the non-Poisson component is not as significant as for earthquakes catalogs with a lower magnitude threshold.

The gamma distribution has been fitted to both earthquake and tsunami source interevent distributions (Corral, 2004; Geist and Parsons, 2008). The light solid line in Figure 2

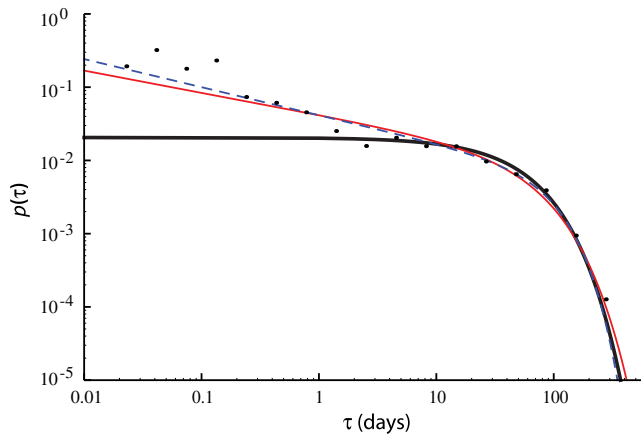


Figure 2. Density distribution of tsunami interevent times from 1960 to 2012 and sizes greater than 0.1 m (filled circles). (Heavy solid line; the best-fit exponential distribution; light solid line, best-fit gamma distribution; dashed line, best-fit generalized gamma distribution.) The color version of this figure is available only in the electronic edition.

represents the gamma distribution with parameters estimated using the maximum-likelihood method. This distribution provides a better fit to the data than the exponential distribution according to the small sample-corrected version of the Akaike Information Criterion (AICc; Burnham and Anderson, 2010), given by

$$\text{AICc} = -2\max_{\theta}(\ln L) + 2K + \frac{2K(K+1)}{n-K-1},$$

in which L is the maximum likelihood, $K = \dim\{\theta\}$ is the number of parameters in the model, and n is the number of samples. Parameter estimates and AICc values are provided for the exponential, gamma, and generalized gamma (dashed line in Fig. 2) distributions in Table 1. In the Results section, the interevent distribution and AICc value from the ETAS model are compared with the distributions shown in Figure 2.

Application of Branching Models to Tsunami Occurrence

Triggering among different tsunami sources is caused by static and dynamic stress changes through the solid earth. Earthquake-to-earthquake triggering often occurs through static stress changes, especially near the source and among

Table 1

Maximum-Likelihood Estimates of Different Interevent Distribution Parameters for the Tsunami Catalog (1960–2012)

Model	Scale (days)	Shape1*	Shape2*	AICc [†]
Exponential	43 (1/λ)			3997
Gamma	64	0.70		3958
Generalized Gamma	97	0.44	1.4	3956

*Shape1 and Shape2 refer to the shape parameters for the gamma and generalized gamma distributions.

[†]Corrected Akaike Information Criterion.

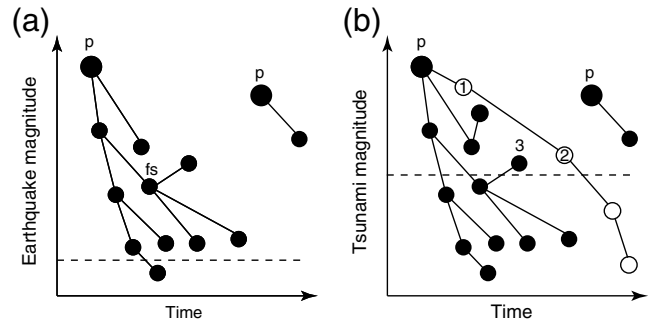


Figure 3. Schematic diagram of temporal branching: (a) earthquakes and (b) tsunamis of different magnitude. Large circles indicate parent events (p). Dashed lines indicate different detection levels by seismic and water-level instruments in (a) and (b), respectively, and fs indicates a foreshock was succeeded by an earthquake of larger magnitude. Events 1, 2, and 3 are discussed in the text. After Kagan (2010) and Geist (2012).

large-magnitude events ($M > 7$; Parsons and Velasco, 2011). Smaller earthquakes can also be triggered by the passage of seismic waves from a parent event (e.g., Prejean *et al.*, 2004; Velasco *et al.*, 2008; Parsons *et al.*, 2014). Triggering of tsunamigenic landslides from parent earthquakes also appears to occur in response to seismic shaking (e.g., ten Brink *et al.*, 2009).

A conceptual branching model for tsunamis (Fig. 3, after Kagan, 2010) is composed of the subset of earthquakes that are tsunamigenic and additional geologic processes such as submarine landslides that result in rapid displacement of the seafloor and overlying water column (open circles in Fig. 3b). Both parent and offspring events linked in the branching process (shown by lines) and isolated spontaneous background events are possible for both earthquakes and landslides. Landslide sources can trigger additional landslide sources, as indicated by a retrogressive landslide sequence (shown by the connected open circles in Fig. 3b; only events 1 and 2 generate tsunamis). A global network of tide gauge stations, ocean-bottom pressure sensors, and eyewitness observations detects tsunamis resulting from earthquakes and landslides (Baptista *et al.*, 1993; Mofjeld, 2009). The detection level for tsunamis limits which events are observed in the branching process (indicated by dashed line in Fig. 3) and is at a higher tsunami magnitude level, calibrated to the earthquake magnitude scale (Abe, 1979, 1995), than for the corresponding earthquakes. Event 3 in Figure 3b is an example of a tsunamigenic event that appears to be spontaneous but is triggered by a preceding event that is below the tsunami detection level. The catalog completeness level is generally at a higher level than the detection level in both cases.

Two types of branching processes have been used to describe the temporal clustering of earthquakes: branching-in-magnitude and branching-in-time processes. The branching-in-magnitude model is consistent with the Gutenberg–Richter magnitude relation and leads to a negative binomial distribution of event counts in a large region and for long time periods (Kagan, 1973b, 2010). This model has been

applied to global tsunami sources by Geist and Parsons (2011), who show that the negative binomial distribution fits the 1890–2010 tsunami catalog with a catalog completeness of 1 m.

The most common branching-in-time model applied to seismicity is the ETAS model. The ETAS model consists of spontaneous background events that produce Poisson distributed offspring. Each of these triggered events can produce offspring of their own according to a Galton–Watson branching process (Daley and Vere-Jones 2003). The background events occur at a stationary Poisson rate, and each of the clusters are independent. Sornette and Werner (2005) provide an alternate interpretation of the ETAS model in which a unique parent (background) event is not defined. Instead, triggered events are conditioned nonlinearly by all other previous earthquakes, weighted by the triggering function. This is a preferable interpretation in the case of tsunami sources. Although ideally displayed as distinct events in Figure 3b, landslide tsunami sources are most often triggered by earthquakes that may or may not themselves be tsunamigenic. Further, successive landslide sources are triggered by both ground shaking (Ozaki *et al.*, 2001) and redistribution of pore pressure (Biscontin *et al.*, 2004; Viesca and Rice, 2012), as well as destabilization from previous landslides, thus presenting a complex feedback among different types of mechanisms.

The ETAS model is based on a Hawkes self-exciting process. The conditional intensity for a point process is defined based on the history of event times $\mathcal{H}_t = \{(t_i, M_i); t_i < t\}$ up to time t as (Ogata, 1999)

$$\lambda(t|\mathcal{H}_t) = \lim_{\Delta t \rightarrow 0} \frac{1}{\Delta t} (\text{One event occurs in } [t, t + \Delta t]|\mathcal{H}_t).$$

The conditional intensity for the Hawkes self-exciting process is given by

$$\lambda(t|\mathcal{H}_t) = \mu + \sum_{i:t_i < t} g(t - t_i),$$

in which $\mu > 0$ is the background rate and $g(t - t_i) \geq 0$ is the triggering function. The triggering function supplies the physical connection among events to explain temporal clustering. For the ETAS model, the triggering function is specified by the Omori–Utsu temporal distribution of aftershocks:

$$\lambda(t|\mathcal{H}_t) = \mu + \sum_{i:t_i < t} \frac{K_i}{(t - t_i + c)^p},$$

in which c represents a limit at which triggered events can be detected (i.e., not a physical property of the earthquake process, Kagan, 2004) and $p > 1$ is an exponent that controls the temporal decay of aftershocks. Parsons (2002) indicates that the Omori–Utsu distribution holds more generally for large globally triggered earthquakes. K_i is the productivity of triggered events and is dependent on the magnitude of earthquake i (Ogata, 1988): $K_i = K_0 e^{\alpha(M_i - M_t)}$, in which K_0 is a normaliz-

ing constant, M_t is a lower magnitude threshold, and α is a coefficient for the magnitude effect on triggering.

For tsunamigenic events, an indicator function is applied to the conditional intensity function described in the previous paragraph. The tsunami indicator is based on a completeness level for the tsunami catalog, according to maximum-per-event tsunami sizes. This completeness level indicates that essentially all tsunamis of this minimum size have been observed for the duration that catalog completeness applies (horizontal bars in Fig. 1). Tsunami size scales approximately with earthquake magnitude, although there is considerable scatter in the observed relationship (Pelayo and Wiens, 1992; Geist, 2012). Therefore, the completeness size associated with the tsunamigenic indicator is roughly linked to the threshold earthquake magnitude M_t in the ETAS model. The inexact relation between tsunami catalog completeness and M_t may be a source of uncertainty in the analysis.

ETAS and other branching models have been applied to study global seismicity (Kagan and Jackson, 1991; Sornette and Werner, 2005; Marzocchi and Lombardi, 2008; Kagan, 2010). Recently, Chu *et al.* (2011) and Lombardi and Marzocchi (2007) apply the ETAS model to study the global occurrence of large earthquakes ($M \geq 5$ and $M \geq 7$, respectively). Chu *et al.* (2011) examine variation in ETAS parameters among different tectonic regimes, whereas Lombardi and Marzocchi (2007) examine nonstationary variations in the rate of large earthquakes. Motivated by these studies, a question that arises is whether ETAS parameters determined from the tsunami catalog, which has a similar magnitude threshold for generation, are consistent with the parameters for large-magnitude, shallow earthquakes? Do subsets of these catalogs that meet tsunamigenic conditions (e.g., beneath oceans, dip slip) need to be considered in order to achieve similarity?

Parameter Estimation

Maximum-likelihood methods are used to estimate the parameters of the temporal ETAS model described in the previous section. The log-likelihood function given in terms of the conditional intensity is (Daley and Vere-Jones, 2003)

$$\ell(\theta) = \sum_i \log[\lambda(t_i|\mathcal{H}_{t_i})] - \int_0^T \lambda(t|\mathcal{H}_t) dt,$$

in which the parameter vector $\theta = (\alpha, c, K_0, p, \mu)$. Computational implementation of this log-likelihood function is given by Ogata *et al.* (1993). Several different optimization methods have been used to numerically determine the maximum of the above log likelihood for a given dataset. A quasi-Newton method was used by Ogata (1988, 1992). More recently, an expectation-maximization method developed by Veen and Schoenberg (2008) has been successfully used in a number of earthquake studies. In this study, a differential evolution method of optimization (Storn and Price, 1997)

appears to provide stable results (see [Appendix](#)), at least for the smaller catalog sizes associated with tsunamis. The likelihood function is also used to determine likelihood profile confidence intervals (CIs) for parameters that are most affected by tsunamigenic conditions. \oplus Residual analysis described by [Ogata \(1988\)](#) using the estimated ETAS parameters for different catalogs and subcatalogs is presented in the electronic supplement available for this paper. Neither the Poisson nor the ETAS models of the tsunami catalog can be rejected using the residual analysis.

When applying the ETAS model to tsunamigenic events, the estimated parameters do not reflect the parameters for earthquakes in general. The conditions for tsunamigenic events, particularly the high magnitude threshold, limit the number of events used in parameter estimation and do not encompass the entire range of earthquake occurrence. The bias imparted by using a high magnitude threshold affects all of the ETAS parameters ([Schoenberg et al., 2010](#)). In addition, [Sornette and Werner \(2005\)](#) indicate the magnitude threshold (M_t) should not be confused with the minimum magnitude that can physically trigger additional events. It is likely that earthquakes below the magnitude threshold contribute to triggered events observed in the catalog that is analyzed (e.g., [Felzer et al., 2002](#)). In the [Discussion](#) section, apparent ETAS parameters estimated under tsunamigenic conditions are compared to those parameters from studies that use a lower threshold magnitude.

Data

Determination of ETAS parameters for tsunamigenic events requires data from both earthquake and tsunami catalogs. Tsunami catalogs include a variety of maximum water level measurements for each event, although the earthquake magnitude scale is inconsistent through the duration of the tsunami catalog. Conversely, earthquake magnitudes are systematically determined in earthquake catalogs, although there is often no or minimal indication of whether a tsunami was generated.

The tsunami catalog used in this study is the NGDC database that compiles tsunami observations from various sources (see [Data and Resources](#)). These observations include instrumental waveform measurements, primarily from tide gauge stations and postevent and eyewitness runup measurements. Two catalog completeness levels are considered: 0.1 and 1.0 m. Microtsunamis that are undetected by coastal measurement systems have been recorded under ideal circumstances on recently deployed ocean bottom pressure sensors ([Hirata et al., 2003](#)). Because these sensors are deployed in deep water, the maximum amplitudes of events will be systematical lower compared to coastal observations and therefore not included in the analysis (unless accompanied by coastal water level measurements).

In addition to tsunami size detection levels, there is also a minimum interevent time in which individual events can be discriminated. Tsunamis measured at coastal tide gauge

stations have a characteristically long coda that obscures successive events ([Geist, 2009](#); [Saito and Furumura, 2009](#); [Saito et al., 2010](#)). Although the e -folding time of the coda is approximately 22 hr in the Pacific basin ([van Dorn, 1984](#)), individual events have been detected with interevent times shorter than several hours. The minimum interevent detection level is unclear; the estimated ETAS c -parameter may help constrain this value. This detection level mainly affects our ability to discriminate sources occurring in close proximity of one another in both space and time. In particular, triggering of landslides from earthquakes often occurs during or soon after shaking, such that individual earthquake and landslide tsunami events are not detected (termed hybrid tsunamis by [Geist, 2001](#)). The 2006 Java tsunami is an example of a hybrid earthquake-landslide tsunami ([Hébert et al., 2012](#)).

The NGDC database includes a field that qualitatively rates the validity of a tsunami event. For this study, only tsunami events with a rating of “definite” or “probable” are used. In addition, only events with origin times of minute precision are used. The latter selection criterion naturally excludes events without an earthquake trigger, such as spontaneous landslide and volcanic tsunamis, because the origin time is not instrumentally recorded. Tsunamis generated by submarine landslides or volcanic processes are included if they are accompanied by an earthquake, which is most often the case.

The earthquake magnitude listed in the tsunami catalog is replaced by the primary magnitude listed in the Centennial catalog ([Engdahl and Villaseñor, 2002](#)) up until 1976 and by the Global CMT catalog from 1976 through 2010. The NGDC tsunami catalog is cross referenced to the NGDC Global Significant Earthquake catalog, which uses M_s or other magnitude scales if an M_w estimate is not available. Because M_s saturates, the primary magnitude listed by the Centennial catalog, corrected to a common reference magnitude scale, provides more accurate and consistent magnitude estimates for the analysis. The Centennial catalog is complete to M_s 7.0 since 1900 ([Engdahl and Villaseñor, 2002](#)). Tsunamis measurable on coastal observation systems usually only occur with a minimum magnitude of approximate M 6.5 ([Ward, 2002](#); [Fig. 4](#)). For this study, only tsunami events associated with earthquakes with a threshold magnitude (M_t) of 7.0 are analyzed as a trade-off between tsunamigenesis and earthquake catalog completeness and at the approximate point where there is a power-law decay in magnitude ([Fig. 4](#)).

The tsunami catalog contains many events cross referenced to lower magnitudes. Some of these magnitudes may be inaccurate, especially for older events. In other cases, the primary tsunamigenic mechanism for some events may not be the earthquake. For example, the 17 March 1952 M 4.5 earthquake (magnitude from NGDC catalog) off the south shore of the island of Hawaii, part of a prolonged earthquake sequence during March and April 1952, generated a 1 m tsunami that swept inland 180 m into a schoolyard ([Macdonald, 1952](#)). It is possible that some undescribed volcanogenic

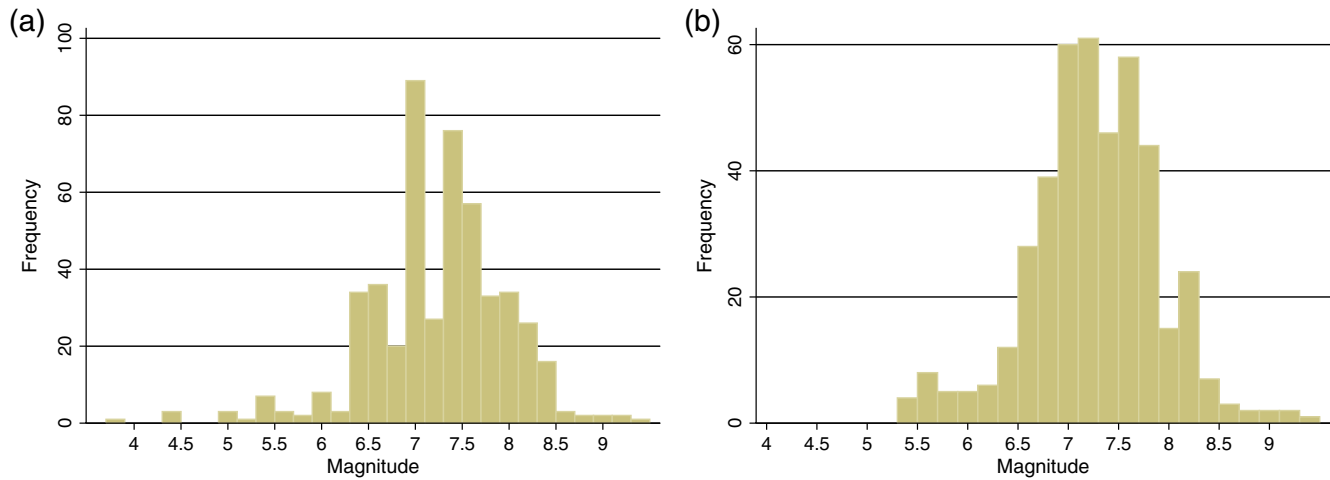


Figure 4. Histograms of earthquake magnitudes for tsunamigenic events from 1960 to 2012 (tsunami sizes > 0.1 m): (a) magnitudes listed in the National Geophysical Data Center tsunami database, and (b) corresponding magnitudes listed in the Centennial catalog. The color version of this figure is available only in the electronic edition.

process that accompanied the earthquake (e.g., submarine landslide) led to the generation of this tsunami (Cox and Morgan, 1977), although the NGDC catalog indicates only an earthquake mechanism was responsible for the tsunami.

Results

Parameters for the ETAS model are estimated for the tsunami catalog according to the two levels of catalog completeness (A_t). At the $A_t = 0.1$ m level, the catalog is complete from approximately 1960, whereas at $A_t = 1.0$ m the catalog is complete from approximately 1900 (Geist and Parsons, 2011; Fig. 1). The maximum-likelihood estimate (MLE) for the ETAS parameters are given in Table 2. The primary result is that the magnitude effect parameter α is diagnostically low in comparison to previous ETAS results from earthquake catalogs. Because α is nearly zero, parameter K_0 governs the productivity of triggered tsunami sources. Comparing the results from the two tsunami catalogs, the mean total rate (λ), and rate of spontaneous events (μ) is, as expected, lower at the $A_t = 1$ m catalog completeness level. The productivity of triggered events is higher for $A_t = 0.1$.

The rate of triggered events compared to the total rate (i.e., $(\lambda - \mu)/\lambda$) is approximately 14% for the $A_t = 0.1$ m catalog and 6.3% for the $A_t = 1.0$ m catalog. This compares to approximately 30% of the worldwide shallow earthquakes $M \geq 7$ being triggered, as calculated from the values listed in

Ogata (1992) and 12% from values in Lombardi and Marzocchi (2007). For shallow subduction zone earthquakes $M \geq 5$, the fractional rate of triggered events is approximately 55% using parameter estimates from Chu *et al.* (2011). This higher rate of triggered events is expected with a lower magnitude threshold. Using single-link cluster analysis, Davis and Frohlich (1991) estimate that 29% of global earthquakes ($m_b \geq 4.8$) belong to a cluster. Overall, the fractional rate of triggered tsunami sources is slightly lower than that of large earthquakes, although still significant.

Saichev and Sornette (2007) derived the interevent distribution associated with the ETAS model. The interevent distribution is based on the Omori–Utsu constants c and θ (for which $p = 1 + \theta$) and the nondimensional parameters $x = \lambda\tau$ and $\varepsilon = \lambda c$:

$$f(x, \varepsilon) = \left[\frac{n\varepsilon^\theta}{x^{1+\theta}} + \left(1 - n + \frac{n\varepsilon^\theta}{x^\theta} \right)^2 \right] \varphi(x, \varepsilon),$$

in which n is the average branching ratio (Helmstetter and Sornette, 2002). $\varphi(x, \varepsilon)$ is a scaling function given by

$$\varphi(x, \varepsilon) = \exp \left[-(1 - n)x - \frac{n\varepsilon^\theta}{1 - \theta} x^{1-\theta} \right].$$

ETAS model interevent distribution is shown in Figure 5 (dashed line) for the 1960–2010 catalog (Fig. 2). The AIC value for the ETAS interevent distribution is 3875, which is

Table 2
Maximum-Likelihood Estimates of ETAS Parameters for Tsunami Catalog at Two Levels of Completeness (A_t).

Tsunami Catalog	N	λ (day $^{-1}$)	μ (day $^{-1}$)	K_0	α	c (day)	p
1900–2010 (1 m)	162	0.0040	0.0038	0.0047	0.064	0.028	1.03
1960–2010 (0.1 m)	224	0.012	0.010	0.011	0.082	0.052	1.03

ETAS, epidemic-type aftershock sequence.

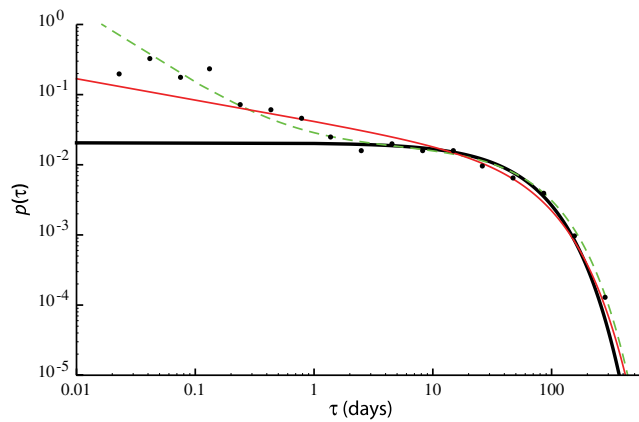


Figure 5. Density distribution of tsunami interevent times from 1960 to 2012 and sizes greater than 0.1 m (filled circles). (Heavy solid line, the best-fit exponential distribution; light solid line, best-fit gamma distribution; dashed line, distribution determined from epidemic-type aftershock sequence parameters.) The color version of this figure is available only in the electronic edition.

lower than the models listed in Table 1, indicating that the ETAS model best describes the data.

The difference between the gamma and ETAS models primarily occurs for short interevent times (<1 day). The ETAS model predicts an abundance of short-interevent times with a higher power-law decay of interevent times. This appears to correspond more closely with the empirical distribution, particularly when recognizing that events with short interevent times and sourced in the same region may be censored by the slowly decaying coda associated with tsunamis. For example, several seismological studies of recent earthquakes indicate that separate subevents occurring on different faults contribute to a single tsunami event as listed in the NGDC catalog (Lay *et al.*, 2010; Harada *et al.*, 2013; Ishii *et al.*, 2013).

Consistency with Earthquake Catalogs

A variety of earthquake catalogs are used to perform parameter estimation for comparison with the results from the tsunami catalog described in the Results section. The Global CMT catalog begins in 1976 with the availability of digital broadband seismic records and is complete to magnitude 5 (Ekström *et al.*, 2012). The period analyzed in this study is from 1976 through 2010 and includes the larger earthquakes in the early twenty-first century and their tsunamigenic aftershocks and triggered events. In addition to the $M \geq 7$ threshold, only earthquake hypocenters shallower than 50 km were analyzed. The theoretical effect of focal depth on the tsunami generation is gradual (Okal, 1988; Geist, 1999); the 50 km cutoff depth used here is determined primarily from empirical evidence (Fig. 6).

Two other additional tsunamigenic conditions were considered. Earthquakes whose epicenters are within ocean boundaries define the first condition. This is a robust and

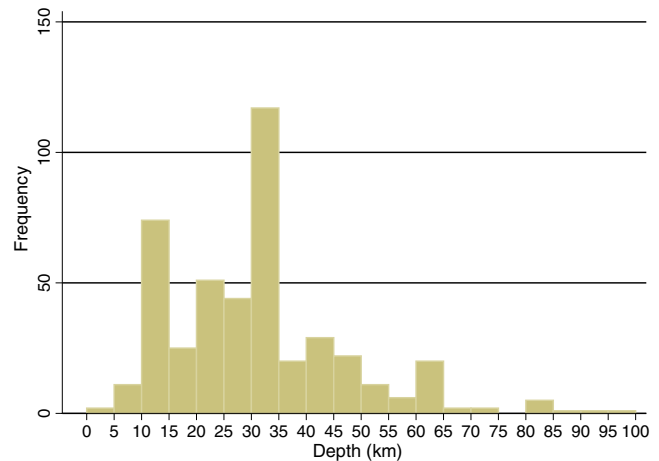


Figure 6. Histogram of earthquake focal depths for tsunamigenic events from 1960 to 2012 (tsunami sizes >0.1 m). The color version of this figure is available only in the electronic edition.

fairly obvious tsunamigenic condition, although coastal earthquakes on occasion can generate tsunamis (Yanovskaya *et al.*, 2003). Also, the epicenter for larger earthquakes in some cases may be located on land, but rupture may extend beneath the oceans. For these reasons, epicenters within 50 km of the coast were accepted.

Another tsunamigenic condition is defined to include only earthquakes with a component of dip slip. For a given seismic moment, dip-slip earthquakes generate larger vertical displacement at the seafloor, and hence larger tsunamis (Yamashita and Sato, 1974; Ward, 1980; Kajiura, 1981; Geist, 1999). Although there is vertical displacement associated with a pure strike-slip earthquake, the small amplitude of the displacement combined with the quadrupole displacement pattern (compared with the dipole pattern associated with dip-slip events) indicates that the associated tsunamis would not reach the recording threshold in most cases. Normal faulting events are defined by a P -axis plunging more than 60° , and thrust events are defined by a T -axis plunging more than 50° following the specifications of Frohlich and Apperson (1992).

All of the aforementioned tsunamigenic conditions are fuzzy in that the magnitude, depth, mechanism, and inland distance limits that constitute the tsunamigenic set are not exact. Accordingly, these conditions applied to earthquake catalogs will result in an imperfect representation of tsunami sources. By comparing the ETAS results between the earthquake and tsunami catalogs, it can be tested whether the temporal occurrence of tsunami sources is captured on average when tsunamigenic conditions are applied.

The Global CMT catalog provides consistent parameter estimation results with respect to the tsunami catalog when taking into account all of the tsunamigenic conditions. Table 3 shows the parameter estimation results for the subcatalog 1 with the magnitude threshold and cutoff depth, followed by subcatalog 2, which adds the submarine condition, and subcatalog 3, which adds the dip-slip constraint.

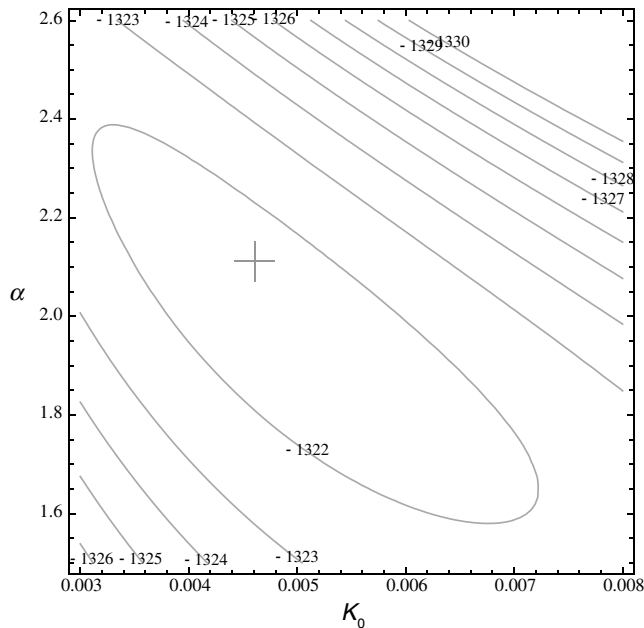


Figure 7. Contour likelihood maps (K_0 , α) for subcatalog 1 of the Global Centroid Moment Tensor (Global CMT) catalog (Table 4). The maximum-likelihood estimate (MLE) is shown by a plus sign.

The parameter estimation results for the tsunami catalog (>0.1 m) are shown on the last row of Table 3 for the same time period as the Global CMT catalog. The catalog length, total rate, and the ETAS parameters (except for p) for subcatalog 3 are each consistent with the tsunami catalog.

The magnitude coefficient of the productivity term (α) is the parameter that appears to be primarily affected by the tsunamigenic conditions. The normalization constant K_0 appears to compensate for the decrease in α by increasing. Omori's parameter p , which controls the temporal decay of triggered events, appears to be significantly closer to 1 for the tsunami catalog than for all of the Global CMT earthquake subcatalogs. Parameter c does not appear to be affected significantly by applying the tsunamigenic criteria listed in Table 3, within the range of uncertainty associated with parameter estimation.

To determine whether the difference in α is significant between the subcatalogs 1 and 3, the profile likelihood CIs are determined, holding the other parameters at their MLEs (Pawitan, 2001). The 95% CIs for α and K_0 are given in Table 4. The differences in parameter α and K_0 between subcatalogs 1 and 3 are significant at the 95% confidence level, although the MLE of K_0 for subcatalog 1 is within the 95% CI of the parameter estimate for the tsunami catalog. The likelihood estimates of α and K_0 are negatively correlated as indicated in Figure 7, consistent with the results of Schoenberg *et al.* (2010).

Results from the other earthquake catalogs using a minimum start year of 1960 are shown in Tables 5 and 6, including the Centennial catalog (2002) and the International Seismological Centre-Global Earthquake Model (ISC-GEM) catalog (Storchak *et al.*, 2013). In addition, results using

the subduction zone earthquake catalog (1982–2008) compiled by Bird and Kagan (2004) are shown in Table 7. In each table, parameter estimation from the tsunami catalog (>0.1 m) for the same time period is shown. Differences in the parameter α between the earthquake and tsunami catalog are similar to those that occur for the Global CMT catalog in Table 3.

Shown in Tables 8 and 9 are longer-duration catalogs starting in 1900 for comparison to the >1.0 m tsunami catalog. The Pacheco and Sykes (1992) catalog (Table 8) includes a letter designation for mechanism. This was used to create subcatalog 3, although quantified criteria could not be used as for the Global CMT catalog. Similar trends in parameter estimates are seen for the larger tsunamis, although the agreement in K_0 between subcatalog 3 and the tsunami catalog is not as good as for the Global CMT catalog. The difference in number of events and rates between subcatalog 3 and the tsunami catalog suggests the minimum threshold magnitude for tsunamigenesis of events >1.0 m is greater than M 7. The number of events and rates are closer using M_t 7.5, although the ETAS parameter estimates are similar to those shown in Table 8 (CIs are larger). The parameter estimates are also shown for the full Centennial catalog in Table 9. $\text{\textcircled{E}}$ For earthquakes catalogs starting in 1900, in most cases the residual analysis indicates that both the stationary Poisson and ETAS models should be rejected, likely because of nonstationary effects (Lombardi and Marzocchi, 2007). In contrast, the two models of the tsunami source catalog, and the Centennial subcatalog $M \geq 2$, starting in 1900 cannot be rejected based on the residual analysis.

Discussion

There is a distinct difference in the estimated ETAS parameters for tsunamigenic events compared to previous studies of global earthquakes. Previous parameter estimates of $M > 7$ shallow global earthquakes are consistent with results presented here, before tsunamigenic conditions are accounted for. The parameters indicated by Ogata (1992) for global $M > 7$ shallow earthquakes over 84 years ($K_0 = 0.0182$, $\alpha = 1.224$, $c = 0.2121$, $p = 1.027$) are most similar to subcatalog 1 of the 1900–2002 Centennial catalog shown in Table 9. The Chu *et al.* (2011) and Lombardi and Marzocchi (2007) studies use the space–time version of the ETAS model (Ogata, 1998). Because of the form of the ETAS model used in Chu *et al.* (2011), it is difficult to directly compare parameter estimates. However, the results from Lombardi and Marzocchi (2007) are consistent with results in this study before applying tsunamigenic conditions. The low values of α estimated for the tsunami catalog and earthquake catalogs with all tsunamigenic conditions applied are significantly lower than those estimated in previous studies of earthquakes; for example, the lowest value in Ogata (1992) is 0.155.

There also appears to be a difference in the temporal decay of tsunami sources (parameter p), with $p \sim 1$ for tsunami

Table 3
Maximum-Likelihood Estimates of ETAS Parameters from Global CMT Catalog (1976–2010)

Subcatalog Criteria	N	λ (day ⁻¹)	μ (day ⁻¹)	K_0	α	c (day)	p
(1) $M \geq 7$, $d \leq 50$ km	281	0.022	0.020	0.0046	2.1	0.12	1.44
(2) (1) and submarine	209	0.016	0.015	0.0064	0.75	0.065	1.41
(3) (2) and dip slip	152	0.012	0.010	0.014	0.049	0.059	1.48
Tsunami catalog	146	0.011	0.0098	0.011	0.082	0.052	1.03

ETAS, epidemic-type aftershock sequence; CMT, centroid moment tensor.

Table 4
95% Confidence Intervals (CI) for ETAS Parameters α and K_0

Subcatalog Criteria	α	95% CI		K_0	95% CI	
(1) $M \geq 7$, $d \leq 50$ km	2.1	1.5	2.4	0.0046	0.0024	0.0068
(2) (1) and submarine	0.75	0.10	1.8	0.0064	0.0045	0.016
(3) (2) and dip slip	0.049	0*	0.75	0.014	0.0064	0.021
Tsunami catalog	0.082	0*	0.86	0.011	0.0036	0.024

ETAS, epidemic-type aftershock sequence.

*Bound of parameter space.

Table 5
Maximum-Likelihood Estimates of ETAS Parameters from Centennial Catalog (1960–2002)

Subcatalog Criteria	N	λ (day ⁻¹)	μ (day ⁻¹)	K_0	α	c (day)	p
(1) $M \geq 7$, $d \leq 50$ km	424	0.028	0.025	0.0077	1.3	0.057	1.18
(2) (1) and submarine	312	0.020	0.018	0.0034	2.1	0.0089	1.15
Tsunami catalog	173	0.011	0.010	0.018	0.79	0.81	1.04

ETAS, epidemic-type aftershock sequence.

Table 6
Maximum-Likelihood Estimates of ETAS Parameters from ISC-GEM Catalog (1960–2009)

Subcatalog Criteria	N	λ (day ⁻¹)	μ (day ⁻¹)	K_0	α	c (day)	p
(1) $M \geq 7$, $d \leq 50$ km	436	0.024	0.020	0.0046	1.4	0.012	1.21
(2) (1) and submarine	328	0.018	0.016	0.0034	2.1	0.0089	1.15
Tsunami catalog	187	0.010	0.0089	0.011	0.082	0.052	1.03

ETAS, epidemic-type aftershock sequence; ISC-GEM, International Seismological Centre-Global Earthquake Model.

Table 7
Maximum-Likelihood Estimates of ETAS Parameters from Subduction Zone Earthquake Catalog (1982–2008; Bird and Kagan, 2004)

Subcatalog Criteria	N	λ (day ⁻¹)	μ (day ⁻¹)	K_0	α	c (day)	p
(1) $M \geq 7$, $d \leq 50$ km	184	0.019	0.017	0.0051	2.0	0.19	1.47
Tsunami catalog	101	0.011	0.0095	0.0011	0.13	0.0027	1.01

ETAS, epidemic-type aftershock sequence.

Table 8
Maximum-Likelihood Estimates of ETAS Parameters from Pacheco and Sykes (1992)
Catalog (1900–1989)

	Subcatalog Criteria	N	λ (day ⁻¹)	μ (day ⁻¹)	K_0	α	c (day)	p
(1)	$M \geq 7, d \leq 50$ km	660	0.020	0.015	0.0099	1.2	0.071	1.00
(2)	(1) and submarine	438	0.013	0.012	0.0074	1.5	0.11	1.20
(3)	(2) and dip slip	151	0.0049	0.0030	0.044	0.046	0.16	1.00
	Tsunami catalog	119	0.0037	0.0035	0.0047	0.064	0.028	1.03

ETAS, epidemic-type aftershock sequence.

Table 9
Maximum-Likelihood Estimates of ETAS Parameters from Centennial Catalog
(1900–2002)

	Subcatalog Criteria	N	λ (day ⁻¹)	μ (day ⁻¹)	K_0	α	c (day)	p
(1)	$M \geq 7, d \leq 50$ km	1149	0.031	0.023	0.015	1.1	0.20	1.03
(2)	(1) and submarine	812	0.022	0.017	0.0098	1.6	0.091	1.06
	Tsunami catalog	147	0.0039	0.0037	0.0074	0.31	0.090	1.01

ETAS, Epidemic-type aftershock sequence.

sources ($A_t = 0.1$ m) and $p > 1.4$ for the Global CMT catalog. Similar differences are observed when comparing the tsunami parameter estimates with parameter estimates from other earthquake catalogs, even for similar numbers of events (subcatalog 3, Table 3). However, $p \sim 1$ has been determined for other, previously published global earthquake studies (Davis and Frohlich, 1991; Ogata, 1992; Lombardi and Marzocchi, 2007). A difference in p -value between the tsunami and earthquake catalogs is not observed for $A_t = 1.0$ m (Tables 8 and 9). The other ETAS parameters, aside from α , estimated from tsunamigenic events fall within the broad range of global and regional studies listed by Ogata (1992) and Helmstetter and Sornette (2002).

Previous studies have detailed the edge effect bias on ETAS parameter estimates, in which parent points are located outside of the sampling window, but offspring points are within the sampling window (Fig. 3b). This can occur by using a catalog of finite duration, but the larger edge effect bias arises from using a magnitude threshold that is much higher than the magnitude of the minimum triggering event. Schoenberg *et al.* (2010) demonstrates an increasing positive bias in c with increasing magnitude threshold and a bias associated with p for all magnitude ranges considered. In addition, Sornette and Werner (2005) indicated significant bias in the apparent fraction of triggered events for large magnitude thresholds. The proportion of spontaneous or background earthquakes (i.e., μ/λ) for all of the catalogs and subcatalogs analyzed here is most certainly artificially high. Earthquakes smaller than M 7 have a significant effect on triggering events larger than this threshold (e.g., Felzer *et al.*, 2002).

Tsunamigenic conditions imposed on the earthquake catalogs greatly reduce the number of events analyzed. To

determine whether the reduction affects the ETAS parameter estimates, random samples of the Global CMT subcatalog 1 (Table 3) are taken, with the number of samples equal to the number of samples in subcatalog 3 ($n = 152$). MLEs were then made for each resampled catalog (Fig. 8). The sampling distribution of α centers near the MLE for subcatalog 1 (mean = 1.7; mode = 1.8). This distribution is consistent with the profile log-likelihood function for α shown by the curve in Figure 8. These results suggest that the low values of parameter α are not simply ascribed to a reduction in the number of events in a subcatalog. Rather, the plunge constraint, and to some degree the submarine location constraint, is removing strong triggering links near parent events. If the

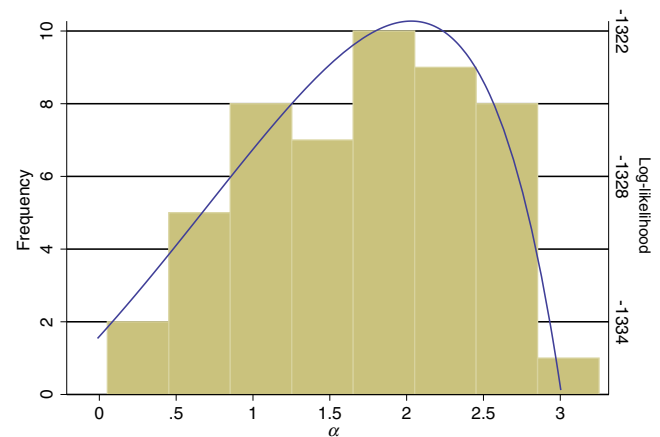


Figure 8. Histogram of MLE α -values for Global CMT subcatalog 1, resampled to 152 events. Fifty resampled subcatalogs were used to create the histogram. The curve is the profile log-likelihood function for α . The color version of this figure is available only in the electronic edition.

focal mechanisms of earthquakes off the parent fault are nearly random and not correlated with the mechanism of the parent earthquake (Kagan, 1992), then the earthquake catalog is no longer uniformly sampled when the plunge constraint is applied.

Consistency in ETAS parameters between tsunami catalogs and earthquake catalogs under tsunamigenic conditions support further application of ETAS and other branching process models to understand the occurrence of tsunami sources. In particular, space–time branching models (e.g., Ogata, 1998) yield geographic specificity to the clustering events, whereas the temporal models used in this study may recognize distant events as part of a cluster. Declustering methods have been developed based on the ETAS model (Zhuang *et al.*, 2002) that may allow the identification of tsunami source sequences within a cluster and test the Poisson process assumption for the parent events (Gardner and Knopoff, 1974; Kagan and Jackson, 1991; Luen and Stark, 2012). Moreover, short-term forecasting methods developed for earthquakes may have significant application for forecasting tsunami events (Kagan and Jackson, 2000, 2010, 2011). Branching process models of seismicity with a much lower magnitude threshold than for tsunamigenesis can be applied to these problems, taking into account tsunamigenic conditions after a model is formulated. Further testing of the accuracy of tsunamigenic conditions applied to earthquake catalogs and application of methods developed in statistical seismology will provide valuable information for understanding tsunami occurrence.

Conclusions

Parameters for the ETAS branching process model were estimated to explain the temporal clustering of tsunami sources. To develop this model, events with magnitudes and origin times of minute precision were needed. These constraints resulted in analyzing only tsunami sources with an earthquake trigger, and not spontaneous landslide or volcanic events. However, examination of the tsunami catalog indicates that most tsunamis generated by landslides or volcanic sources are also accompanied by an earthquake. Therefore, the ETAS model determined in this study is thought to be representative for characterizing tsunami occurrence. Overall, the ETAS model provides a better fit to the observed tsunami source interevent distribution than the Poisson or other temporal clustering models. Results indicate that approximately 14.1% of tsunami events >0.1 m are triggered by other tsunami sources.

The magnitude effect coefficient (α parameter) of ETAS models for tsunami sources is nearly zero, in contrast to ETAS models of global $M \geq 7$ shallow seismicity in which α ranges between 1.5 and 2.4 (95% CI, 1976–2010 Global CMT catalog). This suggests that triggering of tsunami offspring do not depend on the magnitude of the parent event. The low values of α do not seem to be caused by a bias imposed by the reduced number of events in tsunamigenic

subcatalog, although the tsunamigenic criteria do appear to affect the sampling of triggered events.

ETAS parameters are consistent between tsunami sources and earthquakes, when taking into account tsunamigenic conditions. These conditions are approximated by the following criteria: $M \geq 7$, $d \leq 50$ km, submarine epicenter, and component of dip slip (as defined by Frohlich and Apperson, 1992). Although exceptions to these criteria certainly occur for historical tsunamigenic events, they appear to be sufficient to explain the temporal occurrence of global tsunami sources using the ETAS model. The estimated ETAS parameters should be viewed as apparent parameters, owing to the edge effect bias of events occurring outside the sampling window that influence triggering. Nonetheless, the consistency achieved between the tsunami source and earthquake ETAS models indicates that branching process models based on earthquake catalogs can provide the framework for analyzing and forecasting the occurrence of tsunami sources in the future.

Data and Resources

The following databases and catalogs were used for this research: the National Geophysical Data Center Tsunami Event database (http://www.ngdc.noaa.gov/hazard/tsu_db.shtml; last accessed April 2013); the Global Centroid Moment Tensor (CMT) Project database (<http://www.globalcmt.org/CMTsearch.html>; last accessed April 2013); the Centennial earthquake catalog (<http://earthquake.usgs.gov/data/centennial/>; last accessed April 2013); the Pacheco–Sykes earthquake catalog (<http://www.ldeo.columbia.edu/seismology/bigquake/>; last accessed April 2013); the 1982–2008 subduction zone earthquake catalog (subcatalogs of the Global CMT catalog) was searched using http://bemlar.ism.ac.jp/wiki/index.php/Bird's_Zones (last accessed April 2013; now defunct); and the 1977–2002 subduction zone earthquake catalog is available at http://www.seismosoc.org/publications/BSSA_html/bssa_94-6/03107-esupp/index.html (last accessed April 2013).

Acknowledgments

This manuscript greatly benefitted from constructive comments provided by Tom Parsons, two anonymous reviewers, and Associate Editor Ivan Wong. The author also appreciates insightful discussions with Andy Michael regarding the interpretation and applicability of epidemic-type aftershock sequence model results.

References

- Abe, K. (1979). Size of great earthquake of 1837–1974 inferred from tsunami data, *J. Geophys. Res.* **84**, 1561–1568.
- Abe, K. (1995). Estimate of tsunami run-up heights from earthquake magnitudes, in *Tsunami: Progress in Prediction, Disaster Prevention and Warning*, Y. Tsuchiya and N. Shuto (Editors), Kluwer Academic Publishers, Dordrecht, The Netherlands, 21–35.
- Baptista, A. M., G. R. Priest, and T. S. Murty (1993). Field survey of the 1992 Nicaragua tsunami, *Mar. Geodes.* **16**, 169–203.

- Bird, P., and Y. Y. Kagan (2004). Plate-tectonic analysis of shallow seismicity: Apparent boundary width, beta-value, corner magnitude, coupled lithosphere thickness, and coupling in seven tectonic settings, *Bull. Seismol. Soc. Am.* **94**, 2380–2399.
- Biscontin, G., J. M. Pestana, and F. Nadim (2004). Seismic triggering of submarine slides in soft cohesive soil deposits, *Mar. Geol.* **203**, 341–354.
- Burnham, K. P., and D. R. Anderson (2010). *Model Selection and Multimodel Inference*, Second Ed., Springer, New York, 488 pp.
- Chu, A., F. Schoenberg, P. Bird, D. D. Jackson, and Y. Y. Kagan (2011). Comparison of ETAS parameter estimates across different global tectonic zones, *Bull. Seismol. Soc. Am.* **101**, 2323–2339.
- Corral, A. (2004). Long-term clustering, scaling, and universality in the temporal occurrence of earthquakes, *Phys. Rev. Lett.* **92**, doi: [10.1103/PhysRevLett.92.108501](https://doi.org/10.1103/PhysRevLett.92.108501).
- Cox, D. C., and J. Morgan (1977). Local tsunamis and possible local tsunamis in Hawaii, Hawaii Institute of Geophysics, University of Hawaii, 118 pp.
- Daley, D. J., and D. Vere-Jones (2003). *An Introduction to the Theory of Point Processes*, Springer, New York, New York.
- Davis, S. D., and C. Frohlich (1991). Single-link cluster analysis of earthquake aftershocks: Decay laws and regional variations, *J. Geophys. Res.* **96**, 6335–6350.
- Ekström, G., M. Nettles, and A. M. Dziewonski (2012). The Global CMT project 2004–2010: Centroid-moment tensors for 13,017 earthquakes, *Phys. Earth Planet. In.* **200/201**, 1–9.
- Engdahl, E. R., and A. Villaseñor (2002). Global seismicity: 1900–1999, in *International Handbook of Earthquake and Engineering Seismology, Part A*, W. H. K. Lee, H. Kanamori, P. C. Jennings, and C. Kisslinger (Editors), Academic Press, San Diego, California, 665–690.
- Felzer, K. R., T. W. Becker, R. E. Abercrombie, G. Ekström, and J. R. Rice (2002). Triggering of the 1999 M_w 7.1 Hector Mine earthquake by aftershocks of the 1992 M_w 7.3 Landers earthquake, *J. Geophys. Res.* **107**, doi: [10.1029/2001JB000911](https://doi.org/10.1029/2001JB000911).
- Frohlich, C., and K. D. Apperson (1992). Earthquake focal mechanisms, moment tensors, and the consistency of seismic activity near plate boundaries, *Tectonics* **11**, 279–296.
- Gardner, J. K., and L. Knopoff (1974). Is the sequence of earthquakes in southern California, with aftershocks removed, Poissonian? *Bull. Seismol. Soc. Am.* **64**, 1363–1367.
- Geist, E. L. (1999). Local tsunamis and earthquake source parameters, *Adv. Geophys.* **39**, 117–209.
- Geist, E. L. (2001). Reply to comment by E. A. Okal and C. E. Synolakis on “Origin of the 17 July 1998 Papua New Guinea tsunami: Earthquake or landslide?” by E. L. Geist, *Seismol. Res. Lett.* **72**, 367–372.
- Geist, E. L. (2009). Phenomenology of tsunamis: Statistical properties from generation to runup, *Adv. Geophys.* **51**, 107–169.
- Geist, E. L. (2012). Phenomenology of tsunamis II: Scaling, event statistics, and interevent triggering, *Adv. Geophys.* **53**, 35–92.
- Geist, E. L., and T. Parsons (2008). Distribution of tsunami interevent times, *Geophys. Res. Lett.* **35**, L02612, doi: [10.1029/2007GL032690](https://doi.org/10.1029/2007GL032690).
- Geist, E. L., and T. Parsons (2011). Assessing historical rate changes in global tsunami occurrence, *Geophys. J. Int.* **187**, 497–509.
- Harada, T., S. Murotani, and K. Satake (2013). A deep outer-rise reverse-fault earthquake immediately triggered a shallow normal-fault earthquake: The 7 December 2012 off-Sanriku earthquake (M_w 7.3), *Geophys. Res. Lett.* **40**, 4214–4219.
- Hébert, H., P.-E. Burg, R. Binet, F. Lavigne, S. Allgeyer, and F. Schindelé (2012). The 2006 July 17 Java (Indonesia) tsunami from satellite imagery and numerical modelling: A single or complex source? *Geophys. J. Int.* **191**, 1255–1271.
- Helmstetter, A., and D. Sornette (2002). Subcritical and supercritical regimes in epidemic models of earthquake aftershocks, *J. Geophys. Res.* **107**, doi: [10.1029/2001JB001580](https://doi.org/10.1029/2001JB001580).
- Hirata, K., H. Takahashi, E. L. Geist, K. Satake, Y. Tanioka, H. Sugioka, and H. Mikada (2003). Source depth dependence of micro-tsunamis recorded with ocean-bottom pressure gauges; the January 28, 2000 M_w 6.8 earthquake off Nemuro Peninsula, Japan, *Earth Planet. Sci. Lett.* **208**, 305–318.
- Ishii, M., E. Kiser, and E. L. Geist (2013). M_w 8.6 Sumatran earthquake of 11 April 2012: Rare seaward expression of oblique subduction, *Geology* **41**, 319–322.
- Kagan, Y. Y. (1973a). A probabilistic description of the seismic regime, *Izvestiya, Phys. Solid Earth* **4**, 213–219.
- Kagan, Y. Y. (1973b). Statistical methods in the study of seismic processes, *Bull. Int. Statist. Inst.* **45**, 437–453.
- Kagan, Y. Y. (1992). Correlations of earthquake focal mechanisms, *Geophys. J. Int.* **110**, 305–320.
- Kagan, Y. Y. (2004). Short-term properties of earthquake catalogs and models of earthquake source, *Bull. Seismol. Soc. Am.* **94**, 1207–1228.
- Kagan, Y. Y. (2010). Statistical distributions of earthquake numbers: Consequence of branching process, *Geophys. J. Int.* **180**, 1313–1328.
- Kagan, Y. Y., and D. D. Jackson (1991). Long-term earthquake clustering, *Geophys. J. Int.* **104**, 117–133.
- Kagan, Y. Y., and D. D. Jackson (2000). Probabilistic forecasting of earthquakes, *Geophys. J. Int.* **143**, 438–453.
- Kagan, Y. Y., and D. D. Jackson (2010). Earthquake forecasting in diverse tectonic zones of the globe, *Pure Appl. Geophys.* **167**, 709–718.
- Kagan, Y. Y., and D. D. Jackson (2011). Global earthquake forecasts, *Geophys. J. Int.* **184**, 759–776.
- Kajiura, K. (1981). Tsunami energy in relation to parameters of the earthquake fault model, *Bull. Earthq. Res. Inst.* **56**, 415–440.
- Lay, T., C. J. Ammon, H. Kanamori, L. Rivera, K. D. Koper, and A. R. Hutko (2010). The 2009 Samoa-Tonga great earthquake triggered doublet, *Nature* **466**, 964–968.
- Lombardi, A. M., and W. Marzocchi (2007). Evidence of clustering and non-stationarity in the time distribution of large worldwide earthquakes, *J. Geophys. Res.* **112**, doi: [10.1029/2006JB004568](https://doi.org/10.1029/2006JB004568).
- Luen, B., and P. B. Stark (2012). Poisson test of declustered catalogues, *Geophys. J. Int.* **189**, 691–700.
- Macdonald, G. A. (1952). The south Hawaii earthquakes of March and April, 1952, *The Volcano Letter* **515**, 1–5.
- Marzocchi, W., and A. M. Lombardi (2008). A double branching model for earthquake occurrence, *J. Geophys. Res.* **23**, doi: [10.1029/2007JB005472](https://doi.org/10.1029/2007JB005472).
- Mofjeld, H. O. (2009). Tsunami measurements, in *The Sea*, E. N. Bernard and A. R. Robinson (Editors), Harvard University Press, Cambridge, Massachusetts, 201–235.
- Ogata, Y. (1988). Statistical models for earthquake occurrences and residual analysis for point processes, *J. Am. Stat. Assoc.* **83**, 9–27.
- Ogata, Y. (1992). Detection of precursory relative quiescence before great earthquakes through a statistical model, *J. Geophys. Res.* **97**, 19,845–19,871.
- Ogata, Y. (1998). Space-time point-process models for earthquake occurrences, *Ann. Inst. Stat. Math.* **50**, 379–402.
- Ogata, Y. (1999). Seismicity analysis through point-process modeling: A review, *Pure Appl. Geophys.* **155**, 471–507.
- Ogata, Y., R. S. Matsu’ura, and K. Katsura (1993). Fast likelihood computation of epidemic type aftershock-sequence model, *Geophys. Res. Lett.* **20**, 2143–2146.
- Okal, E. A. (1988). Seismic parameters controlling far-field tsunami amplitudes: A review, *Nat. Hazards* **1** 67–96.
- Ozaki, R., S. Takada, and R. E. Kayen (2001). Multi-directional Newmark sliding analysis with compliant materials, *J. Struct. Eng.* **47A**, 571–578.
- Pacheco, J. F., and L. R. Sykes (1992). Seismic moment catalog of large shallow earthquakes, 1900 to 1989, *Bull. Seismol. Soc. Am.* **82**, 1306–1349.
- Parsons, T. (2002). Global Omori law decay of triggered earthquakes: Large aftershocks outside the classical aftershock zone, *J. Geophys. Res.* **107**, 2199, doi: [10.1029/2001JB000646](https://doi.org/10.1029/2001JB000646).
- Parsons, T., and A. A. Velasco (2011). Absence of remotely triggered large earthquakes beyond the main shock region, *Nature Geosci.* **4**, 312–316.

- Parsons, T., M. Segou, and W. Marzocchi (2014). The global aftershock zone, *Tectonophysics* **618**, 1–34.
- Pawitan, Y. (2001). *All Likelihood: Statistical Modelling and Inference Using Likelihood*, Oxford University Press, Oxford, United Kingdom, 528 pp.
- Pelayo, A. M., and D. A. Wiens (1992). Tsunami earthquakes: Slow thrust-faulting events in the accretionary wedge, *J. Geophys. Res.* **97**, 15,321–15,337.
- Prejean, S. H., D. P. Hill, E. E. Brodsky, S. E. Hough, M. J. S. Johnston, S. D. Malone, D. H. Oppenheimer, A. M. Pitt, and K. B. Richards-Dinger (2004). Remotely triggered seismicity on the United States west coast following the M_w 7.9 Denali fault earthquake, *Bull. Seismol. Soc. Am.* **94**, S348–S359.
- Saichev, A., and D. Sornette (2007). Theory of earthquake recurrence times, *J. Geophys. Res.* **112**, doi: [10.1029/2006JB004536](https://doi.org/10.1029/2006JB004536).
- Saito, T., and T. Furumura (2009). Scattering of linear long-wave tsunamis due to randomly fluctuating sea-bottom topography: Coda excitation and scattering attenuation, *Geophys. J. Int.* **177**, 958–965.
- Saito, T., T. Matsuzawa, K. Obara, and T. Baba (2010). Dispersive tsunami of the 2010 Chile earthquake recorded by the high-sampling-rate ocean-bottom pressure gauges, *Geophys. Res. Lett.* **37**, doi: [10.1029/2010GL045290](https://doi.org/10.1029/2010GL045290).
- Schoenberg, F. P., A. Chu, and A. Veen (2010). On the relationship between lower magnitude thresholds and bias in epidemic-type aftershock sequence parameter estimates, *J. Geophys. Res.* **115**, doi: [10.1029/2009JB006387](https://doi.org/10.1029/2009JB006387).
- Sornette, D., and M. J. Werner (2005). Apparent clustering and apparent background earthquakes biased by undetected seismicity, *J. Geophys. Res.* **110**, doi: [10.1029/2005JB003621](https://doi.org/10.1029/2005JB003621).
- Storchak, D. A., D. Di Giacomo, I. Bondár, E. R. Engdahl, J. Harris, W. H. K. Lee, A. Villaseñor, and P. Bormann (2013). Public release of the ISC-GEM global instrumental earthquake catalogue (1900–2009), *Seismol. Res. Lett.* 810–815.
- Storn, R., and K. Price (1997). Differential evolution: A simple heuristic for global optimization over continuous spaces, *J. Global Optim.* **11**, 341–359.
- ten Brink, U. S., H. J. Lee, E. L. Geist, and D. C. Twichell (2009). Assessment of tsunami hazard to the U.S. Atlantic Coast using relationships between submarine landslides and earthquakes, *Mar. Geol.* **264**, 65–73.
- van Dorn, W. G. (1984). Some tsunami characteristic deducible from tide records, *J. Phys. Ocean.* **14**, 353–363.
- Veen, A., and F. P. Schoenberg (2008). Estimation of space-time branching process models in seismology using an EM-type algorithm, *J. Am. Stat. Assoc.* **103**, 614–624.
- Velasco, A. A., S. Hernandez, T. Parsons, and K. Pankow (2008). Global ubiquity of dynamic earthquake triggering, *Nature Geosci.* **1**, 375–379.
- Vere-Jones, D. (1970). Stochastic models for earthquake occurrence, *J. Roy. Stat. Soc., Series B* **32**, 1–62.
- Vere-Jones, D. (1976). A branching model for crack propagation, *Pure Appl. Geophys.* **114**, 711–725.
- Viesca, R. C., and J. R. Rice (2012). Nucleation of slip-weakening rupture instability in landslides by localized increase of pore pressure, *J. Geophys. Res.* **117**, doi: [10.1029/2011JB008866](https://doi.org/10.1029/2011JB008866).
- Ward, S. N. (1980). Relationships of tsunami generation and an earthquake source, *J. Phys. Earth* **28**, 441–474.
- Ward, S. N. (2002). Tsunamis, in *The Encyclopedia of Physical Science and Technology*, R. A. Meyers (Editor), Elsevier, Amsterdam, The Netherlands, 175–191.
- Yamashita, T., and R. Sato (1974). Generation of tsunami by a fault model, *J. Phys. Earth* **22**, 415–440.
- Yanovskaya, T. B., F. Romanelli, and G. F. Panza (2003). Tsunami excitation by inland/coastal earthquakes: The Green function approach, *Nat. Hazards Earth Syst. Sci.* **3**, 353–365.
- Zhuang, J., Y. Ogata, and D. Vere-Jones (2002). Stochastic declustering of space-time earthquake occurrences, *J. Am. Stat. Assoc.* **97**, 369–380.

Appendix

Determining the maximum-likelihood estimate (MLE) for the epidemic-type aftershock sequence (ETAS) model is challenging, owing to the number of parameters, the flatness of the likelihood function for certain parameters, and the possible existence of local maxima (Veen and Schoenberg, 2008). Several global optimization methods were tested to determine the MLE, including random search, Nelder Mead, simulated annealing, and differential evolution. Differential evolution provided the highest likelihood values and least variation using different random seeds. Differential evolution developed by Storn and Price (1997) is a genetic algorithm in which an initial population of parameter vectors is modified according to simple heuristics. For a successive generation, mutant vectors are first formed by the difference between two random vectors. Amplification of the differential variation is controlled by the differential weight ($F \in [0, 2]$). Determination of which parameters in a mutant vector are perturbed is controlled by assigning a uniform random number to the vector elements and selection according the crossover constant ($CR \in [0, 1]$). Storn and Price (1997) indicate that the differential evolution method is well suited where the objective function is flat.

Reasonable physical constraints were imposed on the MLE search. First, it is assumed that μ is not greater than λ . Second, although values of $p < 1$ have been considered in previous studies, p is limited in this study to be > 1 , consistent with the interpretation of the Omori–Utsu law as a probability density (Veen and Schoenberg, 2008). Finally, K_0 , α , and c are all assumed to be greater than or equal to 0.

One thousand optimization searches were performed with different populations of initial parameter vectors controlled by a random seed. In each case, the population size is 50. Values for the differential weight and crossover constant of 0.6 and 0.5, respectively, were used, consistent with the recommendations of Storn and Price (1997). The maximum of the one thousand searches was chosen as the MLE.

U.S. Geological Survey
345 Middlefield Road, MS 999
Menlo Park, California 94025
egeist@usgs.gov

Manuscript received 24 October 2013;
Published Online 1 July 2014